Korean J. Chem. Eng., **31**(8), 1496-1504 (2014)
DOI: 10.1007/s11814-014-0065-8

pISSN: 0256-1115
eISSN: 1975-7220

Development of artificial neural network models for supercritical fluid solvency in presence of co-solvents

Eissa Mohamed El-Moghawry Shokir*,,†, Emad Souliman Al-Homadhi**, Osama Al-Mahdy**, and Ayman Abdel-Hamid El-Midany***

*Faculty of Engineering, Mining, Petroleum and Metallurgical Department, Cairo University, Giza, Egypt
**College of Engineering, Petroleum & Natural Gas Engineering Department, King Saud University, Riyadh, Kingdom of Saudi Arabia
(*Received 24 December 2013 • accepted 21 February 2014*)

Abstract−This paper presents the application of artificial neural networks (ANN) to develop new models of liquid solvent dissolution of supercritical fluids with solutes in the presence of cosolvents. The neural network model of the liquid solvent dissolution of CO_2 was built as a function of pressure, temperature, and concentrations of the solutes and cosolvents. Different experimental measurements of liquid solvent dissolution of supercritical fluids (CO_2) with solutes in the presence of cosolvents were collected. The collected data are divided into two parts. The first part was used in building the models, and the second part was used to test and validate the developed models against the Peng-Robinson equation of state. The developed ANN models showed high accuracy, within the studied variables range, in predicting the solubility of the 2-naphthol, anthracene, and aspirin in the supercritical fluid in the presence and absence of co-solvents compared to (EoS). Therefore, the developed ANN models could be considered as a good tool in predicting the solubility of tested solutes in supercritical fluid.

Keywords: Supercritical, Fluid, Solvents, Cosolvents, Artificial Neural Networks

INTRODUCTION

In the early 19th century, Baron Carniard de la Tour made the first observation of supercritical phase. He mentioned that the boundary between gas and liquid disappeared when the temperature of certain materials was increased in a closed glass container [1,2]. Late 19th century, the solvating power of supercritical fluids was demonstrated by Hannay and Hogart [3] with cobalt (II) chloride, iron (III) chloride, potassium bromide, and potassium iodide-supercritical ethanol systems.

After the sharp increase at the energy cost and governmental regulations for environmental purposes, interest in the supercritical fluid technology has increased as well as the interest in knowledge for high-pressure phase behavior. Every day, there is a new supercritical technology born in the laboratory or pilot plant study is introduced to the industry. Most of the time, applying these technologies is limited due to the lack the phase behavior knowledge of mixtures in the critical region. Therefore, many studies were done for a better fundamental understanding of molecular structure, phase behavior, cosolvent effects, solvation processes between solute and fluid phase, and transport properties of supercritical fluid [2,4].

There are many ways to obtain information about the phase behavior. Although thermodynamic models were introduced to explain fluid behavior at high pressures, at least some experimental data points are necessary to adjust the binary interaction parameters. A wealth of information on the solubility of materials in supercritical fluids has been published in literature [5,6].

Many investigators published different models of solubility behavior of systems involving solid, SCF, and cosolvent; however, all these models were based on their own system. Guha and Madras [7] developed a model that combines the cubic Patel-Teja (PT) EoS with the Wong-Sandler (WS) mixing rule. The model was applied to correlate the solubility of different ternary systems and the corresponding binaries. Only three empirical parameters were required to model the ternary systems, which were the interaction parameter, the hypothetical infinite pressure, activity coefficient, and the interactions between the two solutes. Based on the values of average absolute relative deviation (AARD) obtained, they showed that the model was versatile to predict the solubility of binary and ternary polar and non-polar solutes.

Chafer et al. [8] used two types of thermodynamic models to calculate the solubility of quertecin in supercritical CO_2 and ethanol. One of the models used the group contribution (GC) EoS, while the other used the Soave-Redlich-Kwong (SRK) EoS. They found that the SRK EoS has more capability to correlate the experimental solubility data, but the predictions of the GC-EoS considerably improved when a pressure-dependent parameter was introduced to the model.

Huang, et al. [9] used the Peng-Robinson (PR) EoS to correlate the solubility data of cholesterol and cholesteryl benzoate in supercritical CO_2 in the presence of the polar cosolvents, methanol and acetone. They pointed out that the equation has an advantage in that it provides reasonable estimates of the complex solubility behavior of solids in supercritical CO_2 as a function of temperature and pressure once the required physical properties are known. Berna et al. [10] used the PR EoS and SRK EoS to correlate the solubility data

†To whom correspondence should be addressed.
E-mail: eshokir@gmail.com, shokir05@yahoo.com

for the system composed of catechin, CO_2, and ethanol. They found that both equations gave similar deviations at various conditions of pressure and temperature, but the PR EoS showed better correlations with the experimental points. Chafer et al. [11] arrived at the same conclusion when they used the PR EoS and SRK EoS to correlate the solubility data for the system composed of epicatechin, CO_2, and ethanol.

Yang and Zhong [12] combined the statistical associating fluid theory (SAFT) EoS with a one-parameter mixing rule to evaluate the capability of the SAFT approach for modeling the solubility of solid aromatic compounds in supercritical fluids with cosolvents. This model showed good agreement with the experimental observations with only one temperature-dependent parameter. The results obtained were compared with the Peng-Robinson-Stryjek-Vera (PRSV) EoS combined with the van der Waals one parameter mixing rule, and it was found that the model provides better results than the cubic EoS. The model proved to be useful for the modeling of solids in supercritical fluids with cosolvents.

Bae et al. [13] estimated the solubility of a ternary mixture consisting of supercritical fluid, solute, and cosolvent using an expanded liquid model (Flory-Huggins theory) that considered the supercritical fluid as a liquid phase. The model allows the prediction of the effect of the cosolvent concentration on the solubility of the solute in a supercritical mixed solvent.

Li et al. [14] proposed another solubility model of solids in supercritical fluid with and without cosolvents (for binary and ternary systems) using the solution theory. For the ternary system, the model has four adjustable parameters which are related to the interactions between the molecules in the solution. The model showed better accuracy when compared with the hard-sphere van der Waals 1 (HSVDW1) and hard-sphere van der Waals 2 (HSVDW2) models. However, it is argued in the literature that using regular solution theory to predict the solubility of a solute is only a qualitative approach.

Other models that have been published in the literature include a simplified cluster solvation model by Cheng et al. [15]. Based on studies that reported the formation of clusters or aggregates of the solvent molecules around the solute at high-pressure conditions, they conclude that these clusters should be considered in solid solubility calculations. Therefore, they presented a model that has two temperature independent binary parameters to calculate the solid solubility for binary, multicomponent, and cosolvent systems with various supercritical fluids. For the case of cosolvent, they found that the calculation results were in satisfactory agreement with the experimental data.

Jin et al. [16] used a modification of the Chrastil [17] equation that considered the formation of the solute/cosolvent/solvent complexes and obtained an equation to correlate the solubility of solids and liquids in supercritical CO_2 with cosolvents and mixed cosolvents. They found that the effect on the solubility of each mixed cosolvent lies between those of the two pure cosolvents. Similar results were found when the modified Chrastil [17] model was used by Jin et al. [18] for the measurement of the solubility of propyl *p*-hydroxybenzoate in supercritical CO_2 with pure cosolvents and mixed cosolvents. The effect on the solubility of the mixed cosolvents lies between those of the pure cosolvents.

Therefore, developing high accuracy models of solubility of solids in mixtures of supercritical fluids with cosolvents is highly demanded. Recently, the theory of artificial neural network has found a worldwide approval from those who are concerned with the research in many fields. This may be due to the neural network potentialities in solving problems to which the network is designed, depending on the gained experiences of some similar problems joined with their solutions [19-21]. Hence, our objective is to present an application of neural network to develop a new model of liquid solvent dissolution of supercritical fluids with solutes in the presence of cosolvents, to understanding the solvency process of multicomponent systems and the validation of the developed model against the other early published correlation.

ARTIFICIAL NEURAL NETWORK

Neural network consists of a large number of simple processing elements called *neurons*. Each neuron of the neural network is connected to other neurons by means of directed communication links, each with an associated *weight*, which represents information being used by the net to solve the problem [22]. At the beginning, these connections are assigned independent weighting factors. The input to each node is multiplied by its associated weighting factor and then summed with the product of each of the other input nodes and their respective weighting factors. An activation threshold is then added to this sum, and the result is processed by a non-linear activation function within the node.

There are several types of artificial neural networks [23], the most common of which is the *multilayer perceptron*. Multilayer perceptrons (MLP) consist of groups of interconnected nodes (perceptrons) arranged in layers corresponding to input nodes, hidden nodes and output nodes. The input layer is fed with the input variables and passes them into the hidden layer(s) where the processing task takes place. Finally, the output layer receives the information from the last hidden layer and sends the results to an external source. The network can therefore be interpreted as a form of input/output model, with the weights and threshold as the free parameters of the model. Such networks can model functions of almost any arbitrary complexity, with the number of nodes for the input and output layer defined by the number of data sources as independent variables and dependent variables, respectively. Determining the proper number of nodes for the hidden layers is difficult, and is often determined through experimentation. Too few nodes in the hidden layer impair the network and prevent it from ever correctly mapping inputs to outputs during the training phase; on the other hand, too many nodes impede generalization. In effect, too many nodes allow the network to memorize the pattern (i.e., develop a correlation) presented without extracting the underlying relationship between input and output variables.

The other types of neural network are the generalized regression neural network (GRNN) and probabilistic neural network (PN). These are closely related, with GRNN used for numeric prediction, the PN for category prediction/classification. The GRNN is a three layer neural network with one hidden neuron for each training pattern. The number of neurons in the input layer (first slab) is the number of problem inputs and the number of neurons in the output layer (third slab) matches the number of outputs. The number of neurons in the hidden layer is usually the number of training patterns.

The choice of higher number of hidden neurons may be advantageous in some problems. The GRNN training is achieved by comparing the input pattern in the n dimensional space of all training patterns to determine how far it is from these patterns. The predicted output is proportional to the distance of the given pattern from all training patterns.

BUILDING THE ANN MODELS

This section describes the methodology followed to determine ANN solubility models of anthracene, 2-naphathol, and aspirin in SCF with and without cosolvent, and to estimate the interaction parameters, and to evaluate the effect of the cosolvent concentration on solubility. Throughout this work, the term "solubility" refers to the solute mole fraction in the saturated SCF phase.

1. Data Description

Approximately, 37 experimental data samples for aspirin solubility in SCF with cosolvent of ethanol or methanol at concentrations of 3.0 mol%, and without cosolvent, at different pressure and temperature were collected. Also, 70 data samples of anthracene solubility in SCF with cosolvent of acetone, ethanol, or cyclohexane at concentrations of 4 mol% and without cosolvent were used. Another, 100 data samples for 2-naphathol solubility in SCF with cosolvent of acetone, ethanol, or cyclohexane at concentrations of 3.6 mol%, and without cosolvent were collected. Each data sample is randomly divided into two parts: the first part for neural network training and the second one were put aside to be used for testing the network's integrity and robustness.

2. Network and Architecture

A typical back propagation neural network (BPNN) is composed of three layers: input, hidden, and output layers. Each layer is made up of a number of processing elements or neurons. Each neuron is connected to each neuron in the preceding layer by a simple weighted link. Fig. 1 shows a schematic diagram of the designed BPNN. It has four input neurons that represent n_1 input variables (pressure, temperature, and mole fraction of cosolvents). There are n_2 hidden neurons and one output neuron. The output is the solute solubility. The solid lines represent the strength or weights of the connections between neurons. The number of input and output neurons is usually straightforward and is determined by the particular application. In contrast, the optimum number of hidden neurons is usually obtained by trial and error.

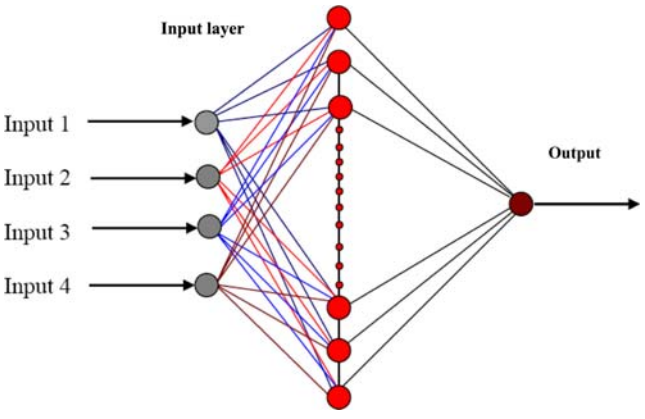

Fig. 1. Schematic diagram of the designed BPNN.

3. Network Training

The BPNN requires the use of training patterns and involves a forward-propagation step followed by a backward-propagation step. The forward propagation step sends an input signal through the neurons at each layer resulting in the calculation of an output value. BPNN uses the following mathematical function:

$$y = f\left[b_o + \sum_{j=1}^{n2} b_j f_j\left(w_{oj} + \sum_{i=1}^{n1} w_{ij} x_i \right) \right] \quad (1)$$

where y is the output variable, x_i are the input variables, b and w are the connection weights, n_1 is the dimension of the input vector, and n_2 is the number of hidden neurons. Note that b_o and w_{oj} are called the bias weights (analogous to the intercept used in statistical regression). Small random numbers are used to initialize all the connection weights (including the bias weights) and the final values are determined by an iterative process. The output, y, depends on the particular transfer function that is chosen. The common transfer functions used in a multiplayer network are log-sigmoid {$y=f(x)=[e^{x/(1+e^x)}]$}. These functions are sometimes called the "squashing function" as it squashes the values into the range of (−1, 1). Therefore, all the values of the input variables (pressure, temperature, and mole fraction of cosolvent) and the dependent target solubility variable must be normalized or scaled in the range of (−1, 1). Consequently, different normalization formulas were tested to normalize the input variables. The following formulation was adapted because it gave a better performance index for the neural network model:

$$X_{new} = [(X - X_{averag})/STDEV] \quad (2)$$

$$X = X_{new}/|(X_{new})_{max}| \quad (3)$$

where: X is the input vector of one dimension for any input variable

The objective of the neural network is to obtain optimal weights to give the best value for the neuron (node of the dependent variable) of the output layer. Three steps are involved in development of a neural network model. The first step is to define the dominant input variables, the number of hidden layers and the number of neurons in each hidden layer. The second is to define a quantitative measure of network performance, called the *performance index*, which is small when the network performs well and large when the network performs poorly. It represents the calculated mean squared error as the difference between the target output, y_S^{real}, and the network output, y_S^{ANN}:

$$e = \frac{1}{q}\sum (y_S^{real} - y_S^{ANN})^2 \quad (4)$$

where q is the number of data in the training set. The third step is to adjust the network weights and biases in order to reduce the performance index. The most common method used to adjust the weights and bias is the back propagation. This method takes the error (difference) from each iteration (training cycle) to change the weights on the neural network interconnections:

$$w_{ij}(t) = \eta \frac{\partial e}{\partial w_{ij}} \alpha \Delta w_{ij}(t-1) \quad (5)$$

where w_{ij} is a weight for the j neuron in the hidden layer i; e is the error from the current training cycle; η is the learning rate (a number

Table 1. Solubility of aspirin in pure CO_2 and/or with cosolvent of 3.0 mol% compared with the measured and predicted values from PR-EOS

CO_2-cosolvent	Pressure (MPa)	Temperature (K)	Solubility, $y_2 \times 10^{-3}$		
			Measured	ANN prediction	PR-EOS
--	12.0	318.10	0.721	0.700	0.790
	17.2	318.10	0.175	0.173	0.176
	20.0	328.15	0.277	0.280	0.310
Ethanol	12.0	318.10	0.938	0.951	0.999
	20.0	318.10	1.520	1.530	1.578
	15.0	328.15	1.280	1.235	1.209
	17.20	328.15	1.490	1.459	1.469
Methanol	10.0	318.10	0.697	0.685	0.715
	17.2	318.10	1.360	1.365	1.456
	15.0	328.15	1.150	1.175	1.187
	20.0	328.15	1.610	1.589	1.659
		AARE		1.65%	4.1%

Table 2. Solubility of 2-naphthol in pure CO_2 and/or with cosolvent of 3.6 mol% compared with the measured and predicted values from PR-EOS

CO_2-cosolvent	Pressure (MPa)	Temperature (K)	Solubility, $y_2 \times 10^{-3}$		
			Measured	ANN prediction	PR-EOS
--	10.05	308.1	7.33	7.42	7.98
	22.05	318.1	13.30	13.54	13.01
	26.00	328.1	17.80	17.79	18.21
Acetone	10.05	308.10	4.83	5.00	4.50
	22.05	308.10	7.06	7.45	7.79
	26.00	308.10	8.16	8.00	8.80
	14.00	318.10	7.66	7.89	7.26
	18.00	318.10	9.77	9.90	9.26
	30.00	318.10	15.00	15.25	16.55
	14.00	328.15	10.70	9.47	9.80
	22.05	328.15	11.00	11.30	12.99
	26.00	328.15	22.3	23	19.55
Ethanol	14.00	308.10	21.70	19.78	23.22
	18.00	308.10	23.60	22.50	25.13
	30.00	308.10	27.70	32.6	28.25
	10.05	318.10	11.50	12.00	12.65
	22.05	318.10	25.70	23.66	27.09
	30.00	318.10	30.20	30.40	31.56
	14.00	328.15	14.90	14.00	13.48
	22.05	328.15	24.30	24.90	26.73
	26.00	328.15	29.30	29.76	30.82
Cyclohexane	14.00	308.10	8.84	8.50	7.69
	26.00	308.10	11.40	11.70	12.54
	30.00	308.10	12.40	12.90	14.01
	18.00	318.10	10.70	11.00	9.94
	22.05	318.10	13.30	12.14	12.48
	26.00	318.10	13.60	14.00	14.96
	14.00	328.15	8.93	9.20	9.82
	22.05	328.15	14.60	14.87	15.62
	30.00	328.15	18.90	19.09	17.84
		AARE		4.08%	7.99%

between 0 and 1 that controls how much the weights can change in each iteration); á is the momentum (a constant on the momentum term that uses the previous weight change to keep the errors changing in the right direction); and t reflects the current iteration (t−1 is the previous iteration).

One of the difficulties that occur during the neural network training is the over-fitting problem. The error on the training set is reduced to a very small value. However, when new data is presented to the network, the error increases. One method for improving generalization is by early stopping. The available data are randomly divided into two groups. The first group is used for the process of network training which represents about 70% of the total sample points. The remaining 30% were used for network testing. Finally, the training process data were divided into two additional groups: validation process (30%) and forward training process (70%). Different numbers of neurons in the first and second neural network layers were tested by testing each time the trained neural network using the testing data points. The correlation coefficients between the predicted and actual solute solubility at different hidden layers and different neuron numbers were recorded each time. The best correlation coefficient between the predicted and actual solute solubility was reached at the optimum number of layers and neurons. The resulting architecture of the neural network to predict aspirin solubility in SCF with 3% mole fraction of ethanol or methanol contained four input variables and one hidden layer with four neurons. In addition, the resulting architecture of the neural network to predict anthracene and 2-Naphathol solubility in SCF with acetone, ethanol and cyclohexane contained five input variables and one hidden layer with seven and nine neurons respectively.

RESULTS AND DISCUSSIONS

The reliability of the ANN for estimating the solute solubility of aspirin in supercritical carbon dioxide modified with 3.0 mol% methanol or 3.0 mol% ethanol at different pressure and temperature was tested using the test data group. Table 1 illustrates that the ANN Aspirin solubility prediction is a close match to the measured values, whereas ANN has average absolute relative error equal to 1.65% compared to 4.1% for PR-EOS.

Table 1 obviously shows that the addition of methanol or ethanol results in a dramatic increase in the solubility of aspirin in supercritical carbon dioxide. As one can see, high aspirin solubility can be easily achieved at low pressures by adding a little methanol or ethanol. The pressure dependence of the cosolvent effect has been explained elsewhere, due to the variation of the local composition around polar solute molecules [24,25]. For cosolvent systems, the polar cosolvent molecules are rich around the polar solute molecule, indicative of favorable cosolvent-solute interactions that turn to result in significant solubility increase. However, the local composition of cosolvent molecules around the solute molecules decreases and gradually approaches that of the bulk solution as pressure increases. That is, the effect of the solute-cosolvent interactions becomes less pronounced as pressure increases. Also, the reliability of the ANN for estimating the solubility of 2-naphthol and anthracene

Table 3. Solubility of anthracene in pure CO_2 and with cosolvent of 4.0 mol% compared with the measured and predicted values from PR-EOS

CO_2-cosolvent	Pressure (MPa)	Temperature (K)	Solubility, $y_2 \times 10^{-4}$		
			Measured	ANN prediction	PR-EOS
	10	308.1	6.66	6.87	7.03
	15	318.1	9.39	9.29	9.43
	25	328.1	12.8	12.67	12.96
Acetone	15	308.10	7.68	7.88	7.20
	25	308.10	9.16	9.43	10.00
	30	308.10	9.56	9.87	10.40
	10	318.10	5.57	5.76	5.01
	15	318.10	9.39	9.51	10.03
	30	318.10	11.90	12.10	12.61
Ethanol	20	318.10	11.50	11.20	12.31
	25	318.10	12.70	12.44	13.53
	30	318.10	13.70	13.40	14.63
	10	328.15	5.22	6.24	4.928
	20	328.15	12.70	11.90	13.46
	25	328.15	14.40	14.15	15.49
Cyclohexane	10	308.10	9.22	9.36	8.67
	15	308.10	11.10	10.78	11.76
	30	308.10	15.10	15.50	16.01
	10	328.15	5.60	5.90	5.10
	20	328.15	14.30	14.31	15.01
	30	328.15	17.80	17.43	19.01
		AARE		3.3%	6.3%

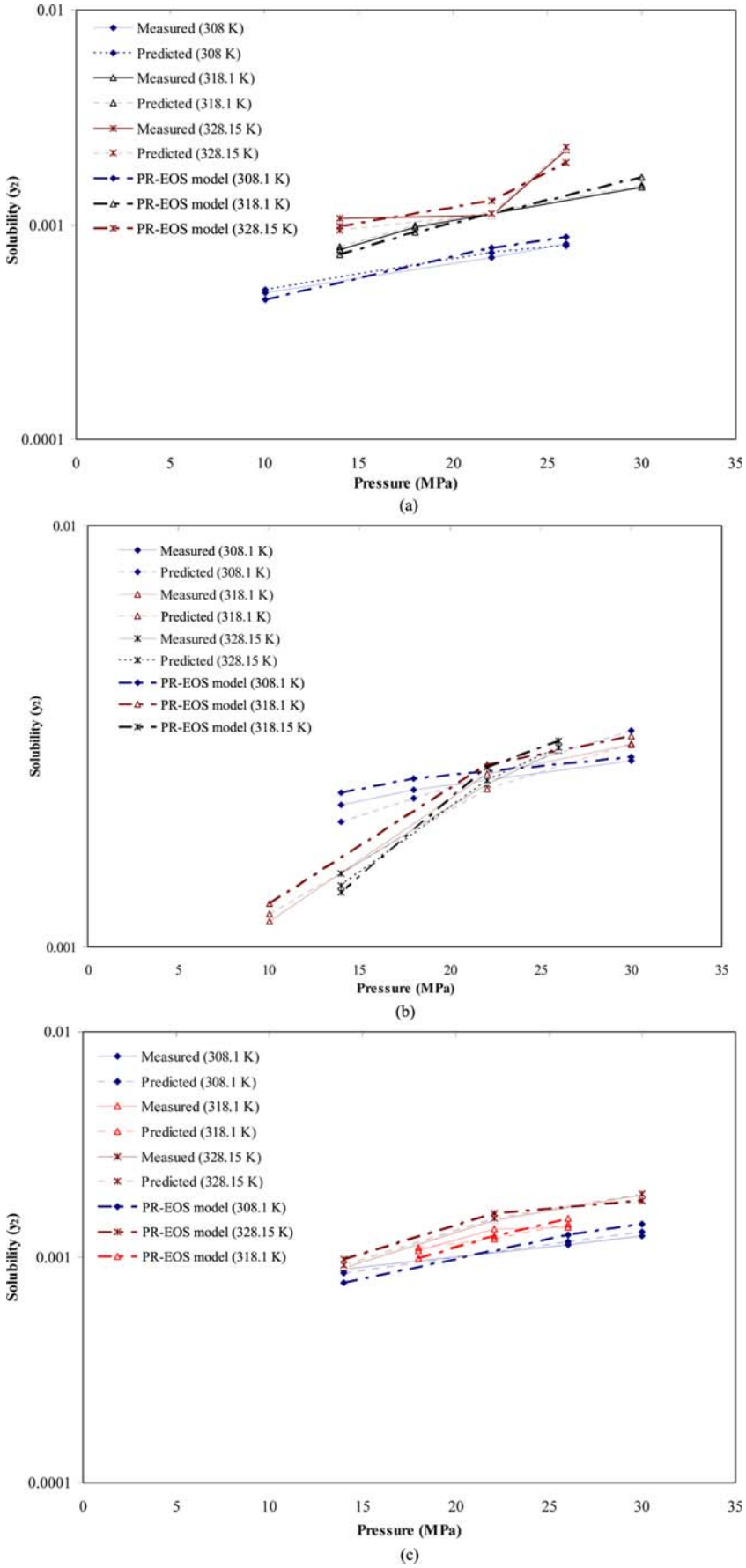

Fig. 2. Solubility of 2-naphthol in SCF with 3.6 mol% cosolvent at 308.1, 318.1, and 328.1 K, (a) acetone, (b) ethanol, and (c) cyclohexane.

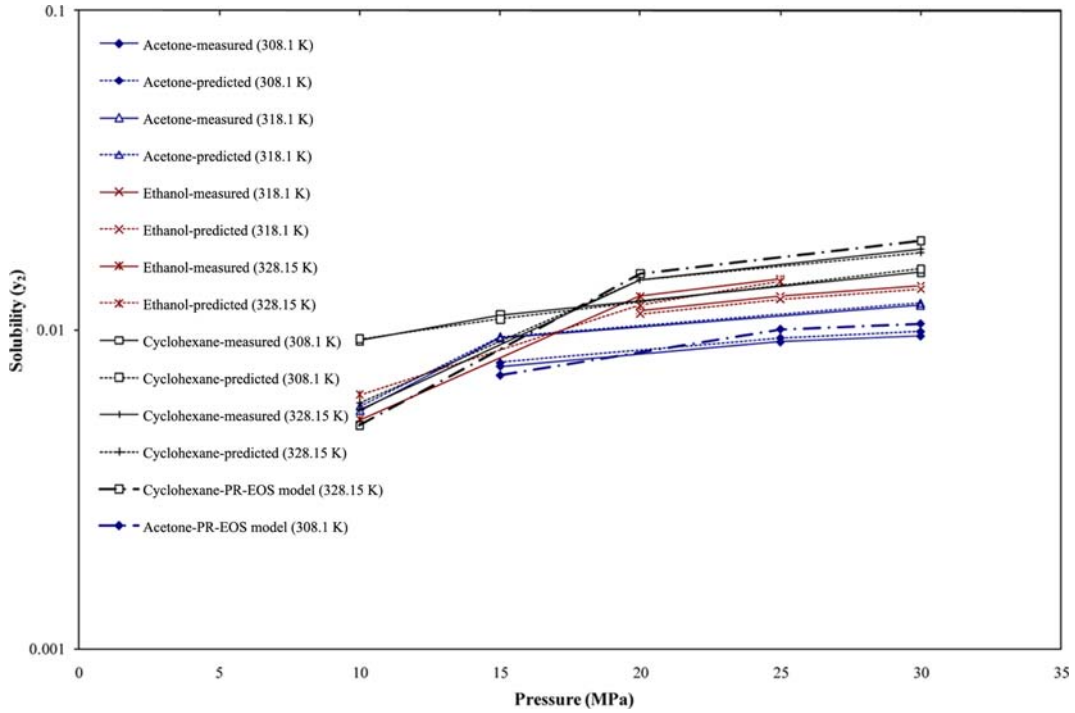

Fig. 3. Solubility of anthracene in SCF with 4 mol% cosolvent at 308.1, 318.1, and 328.1 K, acetone, ethanol and cyclohexane.

in CO_2 with cosolvent (acetone, ethanol or cyclohexane) was further determined using the test data group at different pressure and temperature. Tables 2 and 3 and Figs. 2 and 3 illustrate that the ANN prediction of 2-naphthol and anthracene solubility is a close match to the measured values, whereas ANN has average absolute relative error equal to 4.08% compared to 7.97% for PR-EOS in the case of 2-naphthol, and 3.3% compared 6.3% for PR-EOS in case of anthracene. Figs. 2 and 3 clearly show that increasing the pressure increases the solubility of the 2-naphthol and anthracene in each cosolvent (acetone, ethanol, and cyclohexane); however, the temperature has slight effect on solubility of both 2-naphthol and anthracene.

1. Variable Impact Analysis

The variable impact analysis measures the sensitivity of net predictions to changes in independent variables on training data. As a result, every independent variable is assigned a relative variable impact value. The lower the percent value for a given variable, the less that variable affects the predictions.

The results of the analysis can help in the selection of a new set of independent variables. For example, a variable with a low impact value can be eliminated in favor of some new variables.

However, the results of the impact analysis are relative to a given net. In data sets with smaller numbers of cases and/or larger numbers of variables, the differences in the relative impact of the variables between trained nets may be more pronounced. Fig. 4 is a plot of the impact analysis of independent variables on aspirin solubility in SCF with cosolvent (ethanol and methanol). It indicates a low impact of pressure, high impact of temperature, and approximately the same impact of the ethanol and methanol on the aspirin solubility on SCF. These results confirm and verify the results of Foster et al. [26], Ting et al. [27], and Sauceau et al. [28]. They concluded that the cosolvent effect decreases with the experimental pressure. They stated that for cosolvent systems, the polar cosolvent molecules are rich around the polar solute molecule, indicative of favorable cosolvent-solute interactions that result in significant solubility increase. However, the local composition of cosolvent molecules around the solute molecules decreases and gradually approaches that of the bulk solution as pressure increases.

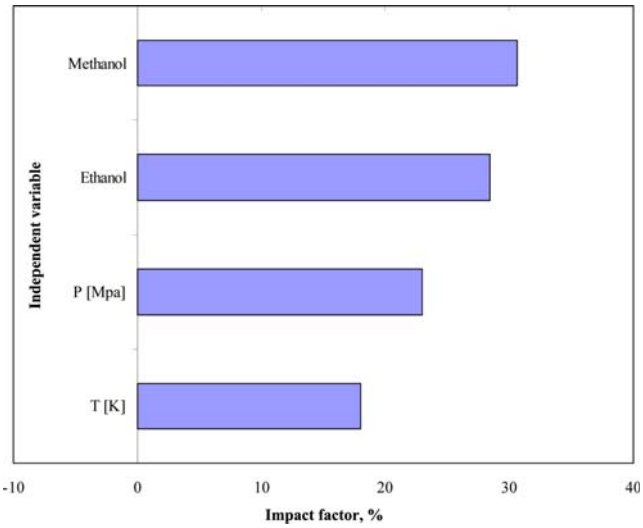

Fig. 4. Variables impacts on the solubility of aspirin in SCF.

In other words, the effect of the solute-cosolvent interactions becomes less pronounced as pressure increases. Figs. 5 and 6 are the plots of the impact analysis of independent variables on the solubility of 2-naphthol and anthracene in SCF with cosolvent (acetone, ethanol and cyclohexane), respectively. The cosolvent effect increases in the order ethanol, acetone, and cyclohexane for 2-naphthol and for anthracene, the order is cyclohexane, ethanol, and acetone. These

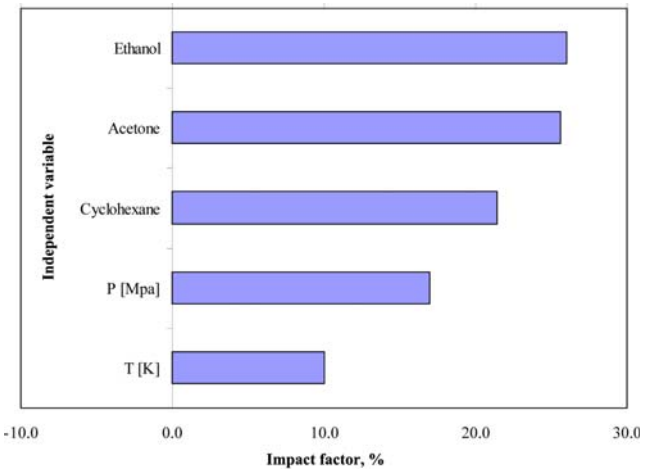

Fig. 5. Variables impacts on the solubility of 2-naphthol in SCF.

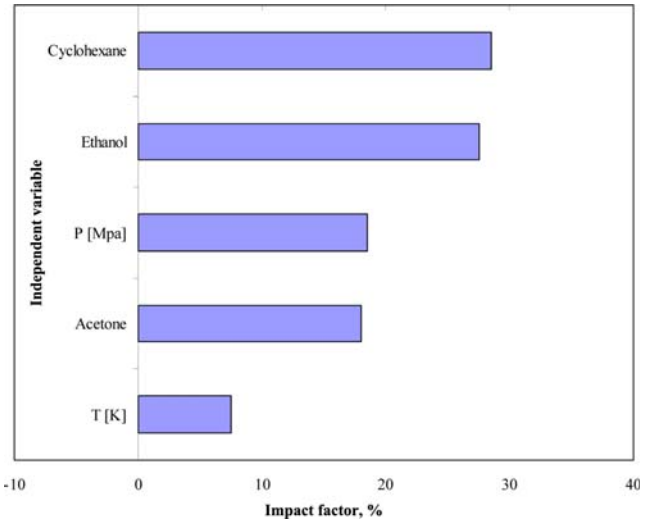

Fig. 6. Variables impacts on the solubility of anthracene in SCF.

results confirmed with the results of Qunsheng et al. [29].

CONCLUSIONS

Artificial neural network is capable of estimating solute solubility with a high accuracy. The ANN model results yielded a good AARE (1.97, 3.8, and 4.6 for predicted aspirin, anthracene, and 2-naphthol, respectively). A low impact of pressure, high impact of temperature and approximately the same impact of the ethanol and methanol on the aspirin solubility in SCF are recorded. Solubility of 2-naphthol and anthracene in supercritical CO_2, with acetone, ethanol or cyclohexane is pronounced. The cosolvent effect on the solubility increases in the order ethanol, acetone, and cyclohexane for 2-naphthol and for anthracene, the order is cyclohexane, ethanol, and acetone.

ACKNOWLEDGEMENT

The authors would like to express their deep appreciation to the deanship of the research center at the College of Engineering, King Saud University for supporting this study (Research Grant 45/429).

NOMENCLATURE

ANN : artificial neural network
BPNN : back propagation neural network
STDEV : standard deviation
b : connection weight of the input layer
b_o : bias weights of the input layer
e : calculated mean square error
K : permeability
n1 : dimension of the input vector
n2 : number of hidden neurons
q : number of training pairs in the training set
t : current iteration
w : connection weight of the hidden layer
w_{ij} : weight for the i neuron in the hidden layer j
w_{oj} : bias weights of the hidden layer
x_i : input variables
X : input vector of one dimension for any input variable
Y : output variable
α : momentum
η : the learning rate
AARE : average absolute relative error, $\frac{100}{N}\sum_{1}^{N}\left|\frac{y_{calculated}-y_{measured}}{y_{measured}}\right|$, %

REFERENCES

1. G. Brunner, *Gas extraction: An introduction to fundamentals of supercritical fluids and the application to separation processes*, Springer, New York (1994).
2. M. A. McHugh and V. Krukonis, *Supercritical fluid extraction: Principles and practice*, Butterworth-Heinemann (1986).
3. J. B. Hannay and J. Hogart, *Proceedings of Royal Society*, **29**, 324 (1879).
4. L. T. Taylor, *Supercritical fluid extraction*, Wiley, New York (1996).
5. R. Dohrn and G. Brunner, *Fluid Phase Equilib. J.*, **106**, 213 (1995).
6. F. Gharagheizi, A. Eslamimanesh, A. H. Mohammadi and D. Richon, *Ind. Eng. Chem. Res*., **50**, 221 (2011).
7. S. Guha and G. Madras, *Fluid Phase Equilib. J.*, **4736**, 1 (2001).
8. A. Chafer, A. T. Fornari, A. Berna and R. P. Stateva, *J. Supercrit. Fluids*, **32**, 89 (2004).
9. Z. Huang, W. D. Lu, S. Kawi and Y. C. Chiew, *J. Chem. Eng. Data*, **49**, 1323 (2004).
10. A. Berna, A. Chafer, J. B. Monton and S. Subirats, *J. Supercrit. Fluids*, **20**, 157 (2001).
11. A. Chafer, A. Berna, J. B. Monton and R.Munoz, *J. Supercrit. Fluids*, **24**, 103 (2002).
12. H. Yang and C. Zhong, *J. Supercritical Fluids*, **33**, 99 (2005).
13. H. Bae, J. Jeon and H. Lee, *Fluid Phase Equilib. J.*, **222**, 119 (2004).
14. Q. Li, C. Zhong, Z. Zhang and Q. Zhou, *Korean J. Chem. Eng.*, **21**, 1173 (2004).
15. K. Cheng, M. Tang and Y. Chen, *Fluid Phase Equilib. J.*, **214**, 169 (2003).
16. J. Jin, C. Zhong, Z. Zhang and Y. Li, *Fluid Phase Equilib. J.*, **226**, 9 (2004).

17. J. Chrastil, *J. Phys. Chem.*, **86**, 3016 (1982).
18. J. Jin, Z. Zhang, Q. Li, Y. Li and E. Yu, *J. Chem. Eng. Data*, **50**, 801 (2005).
19. E. M. El-M. Shokir, Neural Network Determines Shaly-Sand Hydrocarbon Saturation, *Oil Gas J.*, April 23 (2001).
20. E. M. El-M. Shokir, A. Ateeq and A. Al-Sughayer, *J. Can. Pet. Technol.*, **45**, 41 (2006).
21. E. M. El-M. Shokir, H. M. Goda, M. H. Sayyouh and K. Al-Fattah, *Selection and evaluation EOR method using artificial intelligent, SPE Paper 79163 Presented at the 26th Annual SPE International Technical Conference and Exhibition in Abuja*, Nigeria, August 5-7 (2002).
22. L. Fausett, *Fundamentals of neural networks, architectures, algorithms, and applications*, Prentice Hall, Englewood Cliffs, NJ (1994).
23. S. Haykin, *Neural networks: A comprehensive foundation*, Prentice Hall, 2nd Ed. (1998).
24. C. R. Yonker and R.D. Smith, *J. Phys. Chem.*, **92**, 2374 (1938).
25. M. P. Ekart, K. L. Bennett, S. M. Ekart, G. S. Gurdial, C. L. Liotta and C. A. Eckert, *AIChE J.*, **39**, 235 (1993).
26. N. R. Foster, H. Singh, S. L. J. Yun, D. L. Tomasko and S. J. Macnaughton, *Ind. Eng. Chem. Res. J.*, **32**, 2849 (1993).
27. S. T. Ting, S. Macnaughton, D. Tomasko and N. Foster, *Ind. Eng. Chem. Res. J.*, **32**, 1471 (1993).
28. M. Sauceau, J. Letourneau, B. Freiss, D. Richon and J. Fages, *J. Supercrit. Fluids*, **31**, 133 (2004).
29. L. Qunsheng, Z. Zeting, Z. Chongli, L. Yancheng and Z. Qingrong, *Fluid Phase Equilib. J.*, **207**, 183 (2003).